Mugla Journal of Science and Technology

IN SILICO AND DFT ANALYSIS OF A NEW MESO-SUBSTITUTED PORPHYRIN DERIVATIVE

Sümeyye YARALI, Department of Chemistry, Faculty of Science, Mugla Sıtkı Koçman University, Muğla, Turkey, smyyeyarali@gmail.com (0009-0007-8709-882X)
Özgül HAKLI TUTUS*, Department of Chemistry, Faculty of Science, Mugla Sıtkı Koçman University, Muğla, Turkey, ozgulhakli@mu.edu.tr (https://orcid.org/0000-0001-9316-2444)
Onur GENÇ, Department of Physics, Faculty of Science, Aydın Adnan Menderes University, Aydın, Turkey, onur.genc@adu.edu.tr (https://orcid.org/0000-0002-9061-7519)
Şerife Gökçe ÇALIŞKAN*, Department of Physics, Faculty of Science, Aydın Adnan Menderes University, Aydın, Turkey, gcaliskan@adu.edu.tr (https://orcid.org/0000-0001-5421-3472)
Nursabah SARIKAVAKLI, Department of Chemistry, Faculty of Science, Aydın Adnan Menderes University, Aydın, Turkey, nsarikavakli@adu.edu.tr (https://orcid.org /0000-0002-9359-7672)

Received: 16.09.2024, Accepted: 31.10.2024
Research Article
*Corresponding author
DOI: 10.22531/muglajsci.1551084

Abstract

In this study, we synthesized and characterized a novel unsymmetrical meso-aryl substituted porphyrin derivative. Comprehensive structural elucidation was achieved using a suite of spectroscopic techniques, including ^{1}H and ^{13}C Nuclear Magnetic Resonance (NMR), Fourier-Transform Infrared (FT-IR) spectroscopy, and Ultraviolet-Visible (UV-Vis) spectroscopy. To further investigate the compound's potential therapeutic applications, in silico studies were performed, focusing on its interactions with breast cancer-associated target receptors, specifically the epidermal growth factor receptor (EGFR) and insulin-like growth factor receptor (IGFR), through molecular docking simulations. Additionally, bioactivity properties were evaluated via absorption, distribution, metabolism, and excretion (ADME) analysis. Complementary to the experimental work, Density Functional Theory (DFT) calculations at the B3LYP/6-311G+(d,p) level were conducted to optimize the molecular structure and determine key quantum chemical parameters, such as the highest occupied molecular orbital (HOMO) and lowest unoccupied molecular orbital (LUMO) distributions. These computational insights provide a deeper understanding of the electronic characteristics and reactivity of the synthesized compound, highlighting its potential for further development as a cancer therapeutic agent.

Keywords: Porphyrin, DFT analysis, Molecular docking, ADME analysis

YENİ BİR MESO-SUBSTİTÜE PORFİRİN TÜREVİNİN İN SİLİKO VE DFT ANALİZİ

Özet

Bu çalışmada, yeni bir asimetrik meso-aril substitüe porfirin türevi sentezlenmiş ve karakterize edilmiştir. Yapısal özellikler, ^{1}H ve ^{13}C Nükleer Manyetik Rezonans (NMR), Fourier Dönüşümlü Kızılötesi (FT-IR) spektroskopisi ve Ultraviyole-Görünür (UV-Vis) spektroskopisi dahil olmak üzere bir dizi spektroskopik teknik kullanılarak kapsamlı bir şekilde ortaya konmuştur. Bileşiğin potansiyel terapötik uygulamalarını araştırmak amacıyla, meme kanseri ile ilişkili hedef reseptörler olan epidermal büyüme faktörü reseptörü (EGFR) ve insülin benzeri büyüme faktörü reseptörü (IGFR) ile etkileşimlerini incelemek için moleküler yerleştirme simülasyonları kullanılarak in silico çalışmalar gerçekleştirilmiştir. Ayrıca, bileşiğin biyolojik aktivite özellikleri absorpsiyon, dağılım, metabolizma ve atılım (ADME) analizi ile değerlendirilmiştir. Deneysel çalışmalara ek olarak, B3LYP/6-311G+(d,p) seviyesinde Yoğunluk Fonksiyonel Teorisi (DFT) hesaplamaları gerçekleştirilmiş ve moleküler yapının optimize edilmesi ve en yüksek dolu moleküler orbital (HOMO) ile en düşük boş moleküler orbital (LUMO) dağılımları gibi temel kuantum kimyasal parametrelerin belirlenmesi sağlanmıştır. Bu hesaplamalı veriler, sentezlenen bileşiğin elektronik özelliklerini ve reaktivitesini daha iyi anlamamıza katkıda bulunarak, kanser terapötik ajanı olarak geliştirilmesi için potansiyelini vurgulamaktadır.

Anahtar Kelimeler: Porfirin, DFT analizi, Moleküler docking, ADME analizi

Cite

Yaralı, S., Tutus Haklı, Ö., Genç, O., Çalışkan, Ş.G., Sarıkavaklı, N., (2024). "*In Silico and DFT Analysis of a New Meso-Substituted Porphyrin Derivative*", Mugla Journal of Science and Technology, 10(2), 42-51.

1. Introduction

Porphyrins are known as "pigments of life" due to their biological importance [1-8]. Examples of iron, magnesium, and cobalt complexes of porphyrin compounds can be given. Iron-complexed porphyrin compounds form hemoglobin, myoglobin, and cytochrome oxidase. They play a role in oxygen transport, oxygen storage, electron transport, and oxygen reduction, respectively. Magnesium-complexed porphyrin compounds, such as chlorophyll, enable energy conversion in plants, from light to energy. Cobalt-complexed porphyrin compounds include Vitamin B12, essential for protein synthesis, carbohydrate and fat metabolism [9-12]. The etymology of "porphyrin", which is from the Greek word "Porphyra", meaning dark purple or violet color, dates back to ancient Greece. Porphyrins consist of four interconnected four pyrrole rings by a methine (=CH2-) bridge [13, 14]. Nitrogen atoms bonded to the pyrrole in the interior of the molecule accept protons with the unshared electron pair on the nitrogen atom and form the dicationic structure. The other two nitrogens donate protons to form the dianionic structure [2]. The porphyrin molecule is aromatic. Its aromaticity is as follows: n=4 in the 4n+2 delocalized π-electron system. Although it contains 22 π-electrons, 18 of these electrons are delocalized according to the Hückel rule. [15].

Meso-substituted porphyrins have the following advantages: 1. Tuning of the physicochemical and photobiological properties of the photosensitizer, which is relevant for the biochemical and physiological properties of the target. 2. Allowing precise tuning of its distribution between subcellular or sub tissue compartments. [16].

Cancer...It occurs when cells multiply abnormally. The main cause of cancer-related deaths is the metastasis of cancer cells. Therefore, early detection of cancer is very important. Porphyrin molecules have been shown to exhibit greater inhibitory activity against cancer cells than against normal cells [17-19]. Chemotherapy and radiotherapy are treatment methods used in cancer therapy. Chemotherapy, which is effective in cancer treatment, has various side effects. Therefore, researchers aim to develop targeted and less toxic new drugs due to these side effects [20]. Lately, scientists have turned their gaze towards creating novel medications that are safer, more potent, less intrusive, and economical, while also being resilient against resistance development through innovative mechanisms. Porphyrins and their derivatives have emerged prominently among various categories of new pharmaceuticals, with their medical uses documented over several decades. Porphyrins, as mentioned above, are nitrogen-containing heterocyclic compounds ubiquitous in biological systems. In addition to playing critical roles such as transporting and storing electrons and oxygen, they function as catalytic centers in biotransformation processes, similar to enzymes like cytochrome P450. [21-23].

In this study, the synthesis of unsymmetrical porphyrin derivative was reported. This derivative was designed to contain tertiary butyl groups attached to three phenyl rings as an aryl group in the meso position. Tertiary butyl groups contribute to increasing the solubility of the molecule. In the fourth phenyl group, there is an epoxy chain containing chlorine in the para position. Moreover, porphyrins have the ability to selectively accumulate in cancer cells. This selective accumulation is primarily due to the π-π stacking interactions between the π-conjugated structure of porphyrins and the aromatic amino acid residues of blood proteins, such as albumin, LDL, and transferrin. Additionally, receptor-mediated endocytosis of these proteins, which is enhanced in cancer cells, further facilitates porphyrin uptake. Based on existing literature, our goal is to evaluate the biocompatibility of the porphyrin molecule and its potential to mitigate the side effects of anticancer agents [24]. To achieve this, ADME analysis was conducted to predict bioactivity descriptors, and molecular docking was used to provide insights into interactions between the new compound and potent receptors responsible for breast cancer, such as the epidermal growth factor receptor (EGFR) and insulin-like growth factor receptor (IGFR). Furthermore, the geometry of the synthesized compound was optimized and analyzed employing density functional theory (DFT), and various electronic properties were determined.

Considering the information provided earlier, our investigation delves into an unsymmetrical meso-aryl substituted porphyrin derivative, scrutinizing its attributes through molecular docking, DFT, and assessing its bioactivity properties.

2. Materials and Methods

All chemicals were obtained commercially (Aldrich or Merck). They were used without purification. The molecular structure was characterized by FT-IR, ^{1}H NMR, ^{13}C NMR, and UV-Vis. $CDCl_3$ was used as a solvent in the NMR spectrum. Chemical shifts are given as ppm (parts per million) from tetramethylsilane.

2.1.Synthesis

2.1.1.Synthesis of 4-(2-(2-(2-(2 Chloroethoxy)ethoxy) ethoxy) ethoxy) benzaldehyde

Synthesis of aldehyde compound is done according to reference. (Figure 1). Briefly, 4- hydroxybenzaldehyde (8 g, 6.55x10-2 mol), Bis[2-(2-chloroethoxy)ethyl]ether (13.45 ml, $6.87x10^{-2}$ mol), K_2CO_3 (9.05 g, $6.55x10^{-2}$ mol) and dry DMF (100 mL) were added to the 2-necked flask. The reaction mixture was stirred at 105°C were added directly as a raw material for the next step (Figure 1) [25].

2.1.2. 5,10,15-Tris(4-(tert-butyl)phenyl)-20-(4-(2-(2-(2-(2-chloroethoxy)ethoxy)ethoxy)ethoxy) phenyl) porphyrin

4-tertbutylbenzaldehyde (75 mmol) and the 4-(2-(2-(2-(2-chloroethoxy)ethoxy)ethoxy)ethoxy)benzaldehyde were dissolved in propionic acid (240 mL). It was stirred (30 minutes at 60°C). Pyrrole (105 mmol) was added dropwise to the reaction mixture, which was then refluxed for 2 hours.

After cooling to room temperature (b.p. 141.2 °C), two-thirds of the propionic acid was removed. Methanol (250 mL) was subsequently added, and the solution was left to cool overnight in the refrigerator. The resulting purple solid was collected by filtration and purified using column chromatography with dichloromethane (DCM) as the elution solvent (Figure 1) [26]. 5,10,15-Tris(4-(tert-butyl)phenyl)-20-(4-(2-(2-(2-(2-chloroethoxy)ethoxy)ethoxy)ethoxy) phenyl) porphyrin was synthesized (Figure 2). The mechanism of synthesis is shown in Figure 1. FT-IR-ATR (cm^{-1}): N-H (3316.06), C=C (1463.27), C=N (1346.25), C-O (1166.17), C-N (1042.58), 973.11 (N-H), 724.76 (oop N-H). ^{1}H NMR (400 MHz, $CDCl_3$): δ, ppm 8.90 (d, 8H, β-pyrrole-**H**), 8.13 (d, 2H, phenyl-**H**), 7.83 (t, 6H, phenyl-**H**), 7.65 (t, 6H, phenyl-**H**), 7.35 (dd, 2H, phenyl-**H**), 4.44 (t, 2H, phenyl-O-**CH_2**), 4.07 (t, 2H, Cl-**CH_2**), 3.89 (t, 2H, **CH_2**), 3.82 (t, 2H, **CH_2**-CH_2-Cl), 3.78 (s 8H, O-**CH_2-CH_2**-O-**CH_2-CH_2**), 1.28 (s, 27H, CH_3) -2.78 (s, 2H, pyrolic **NH**) ^{13}C NMR (400 MHz, $CDCl_3$), δ, ppm: 158, 143.4, 135.5, 127.77, 127.64, 120.3, 120.1, 119.8, 119.6, 113.5, 112.8, 71.4, 70.9, 70.8, 70.7, 70, 55.5, 42.8, 29.7. $C_{64}H_{69}ClN_4O_4$. UV-Vis: 650 nm (Q-band), 592 nm (Q-band), 552 nm (Q band) 515.5 nm (Q band), 419.5 nm (Soret band).

Two different aldehyde molecules were used for the synthesis of the porphyrin derivative molecule. The synthesis mechanism was drawn considering the reference as shown in Figure 2 [27].

The aldehyde functional group is protonated by the proton of the acid in the medium. Electron flow starts from the unshared electron pair on the oxygen in the carbonyl group. The proton is captured. The unshared electron pair is used to form bonds with hydrogen. In this way, the oxygen in the carbonyl group is protonated.

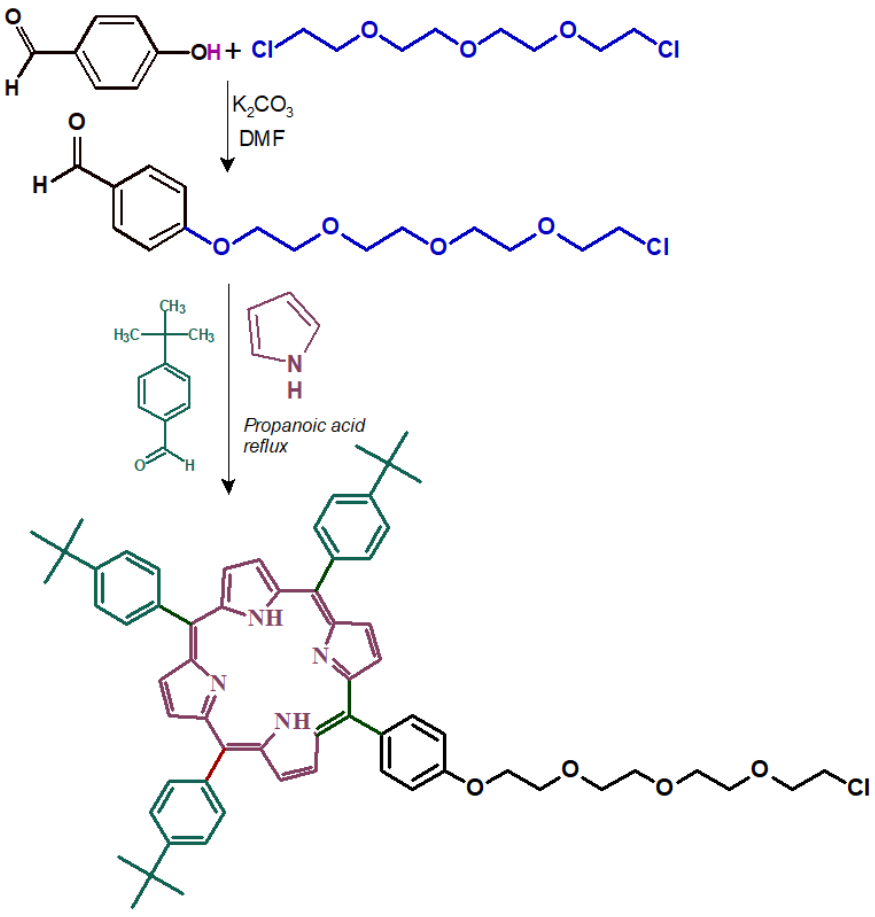

Figure 1. Preparation of 5,10,15-Tris(4-(tert-butyl)phenyl)-20-(4-(2-(2-(2-(2-chloroethoxy)ethoxy)ethoxy)ethoxy) phenyl) porphyrin

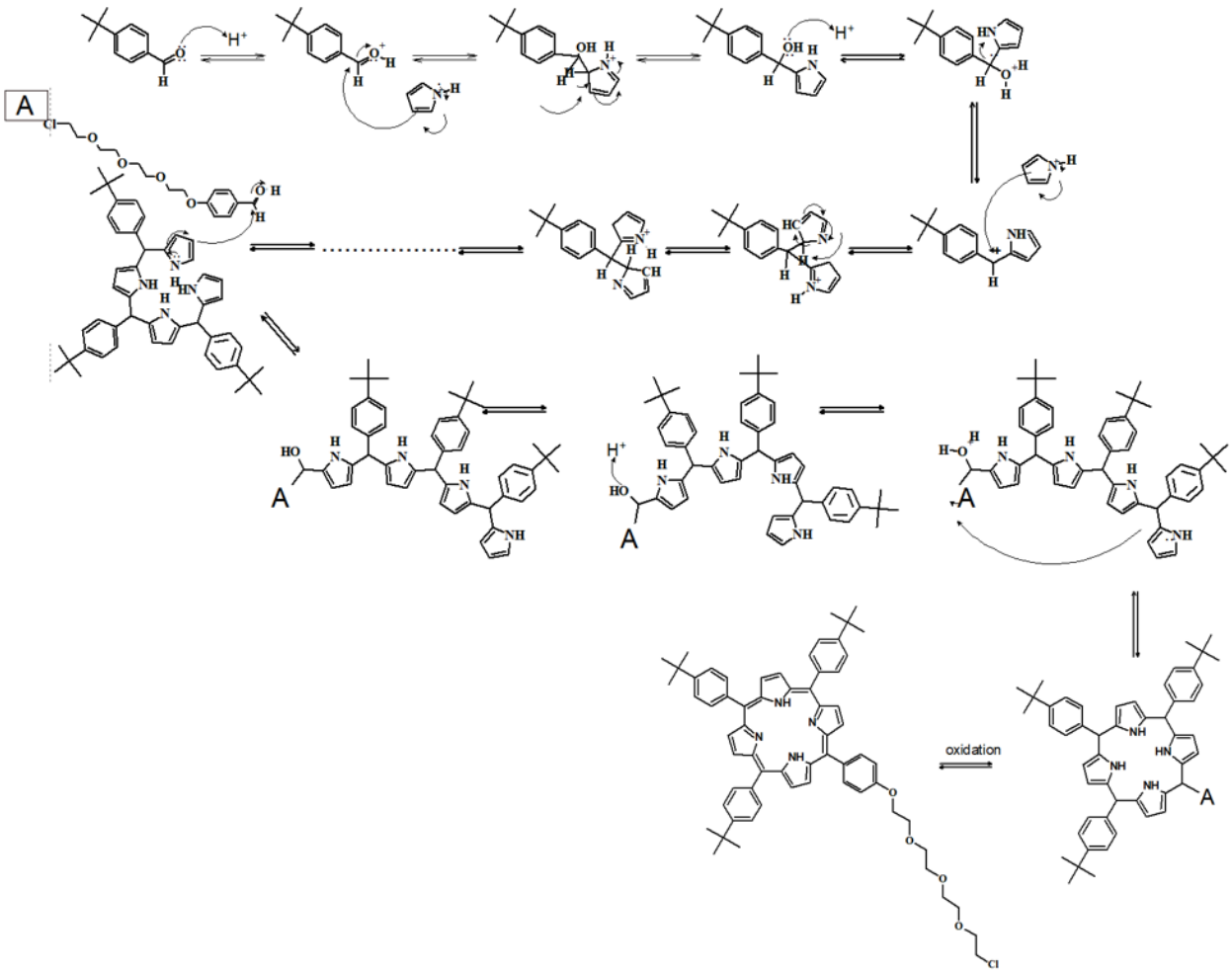

Figure 2. Mechanism of porphyrin synthesis

The unshared electron pair on oxygen is now two. There is a (+) charge on oxygen. He made three bonds. The π bond electrons, which are the electron source in the pyrrole ring, attack the electropositive carbonyl carbon and the π bond between the carbon and oxygen in the carbonyl opens on the oxygen. The bond electron turns into an unshared electron pair. There is a carbon bridge between dearomatic pyrrole and phenyl rings. Hydroxyl (OH) is attached to this carbon. The OH group is protonated by the acid proton and turns into H_2O, which is an easily leaving group. H_2O leaves, releasing its bond electrons, and the bond electrons fold between the bridge carbon and the pyrrole carbon, forming a π bond. The mechanism is repeated in this way using a total of four pyrroles and a porphyrin derivative molecule is obtained. Aldehyde groups are changed according to the derivative desired to be obtained.

2.2. In Silico Studies

2.2.1 Molecular Docking

Docking studies were conducted to investigate the binding mechanisms of the newly synthesized compound with the EGFR (PDB ID: 1M17) and IGFR (PDB ID: 3I81). The 3D structures of the target proteins were sourced from the RCSB Protein Data Bank. For the preparation of these proteins, water molecules were eliminated, and polar hydrogen atoms along with Kollman charges were introduced using AutoDock Tools 1.5.7 (ADT, The Scripps Research Institute, La Jolla, CA, USA).

The compound was prepared for docking by first generating its 2D structure using ChemSketch software. Subsequently, a 3D structure was generated and optimized to achieve the minimum energy value. The optimized structure was then converted to PDB format using Avogadro software. Autodock Vina [28] was utilized to dock the compound onto the EGFR and IGFR target proteins. The grid box covered the binding region of the target protein with 100 x 100 x 100 Å grid points which were separated by 0.375 Å. For EGFR and IGFR, the 3D coordinates were set to 23.553 x 9.725 x 59.329 and 8.136 x 0.106 x 17.702, respectively. Autogrid utility of AutoDock was used for this process. The complex that occurred between the ligand and protein was visualized using DS Visualizer Software. In addition, for validation of the molecular docking approach, we selected the ligands erlotinib and 1-{4-[(3-cyclopropyl-1H-pyrazol-5-yl)amino]pyrrolo[2,1f][1,2,4]triazin-2-yl}-N-(6 fluoropyridin-3-yl)-2-methyl-L-proli namide which were attached to the structure of EGFR and IGFR target

proteins respectively as positive controls and performed molecular docking analysis using the similar parameters.

2.2.2. ADME Analysis

The bioactivity scores of a new unsymmetrical meso-aryl substituted porphyrin derivative were assessed using the www.molinspiration.com [29] website. The SMILES notations of the compounds were obtained using ChemDraw software. The bioactivity parameters were determined by uploading the SMILES notation of the compound to the www.molinspiration.com website.

2.2.3. DFT Studies

The optimization of a novel unsymmetrical meso-aryl substituted porphyrin was carried out using Gaussian 09 software [30]. This optimization process applied full relaxation on the potential energy surfaces at the B3LYP/6-311G+(d,p) level of Density Functional Theory (DFT). Vibrational analysis was performed to verify that the optimized structures represented local minima on the energy surface. After the optimization, frontier molecular orbitals (FMOs) were evaluated, specifically the highest occupied molecular orbital (HOMO) and the lowest unoccupied molecular orbital (LUMO). The energy gap was calculated as the difference between the HOMO and LUMO energies. Furthermore, various chemical reactivity descriptors, such as electronegativity (χ), chemical potential (π), global hardness (η), global softness (σ), and global electrophilicity (ω), were determined based on equations (1-5).

$$\chi = -\frac{1}{2}(E_{HOMO} + E_{LUMO}) \quad (1)$$

$$\eta = -\frac{1}{2}(E_{HOMO} - E_{LUMO}) \quad (2)$$

$$\pi = \frac{1}{2}(E_{HOMO} + E_{LUMO}) \quad (3)$$

$$\sigma = \frac{1}{\eta} = -\frac{2}{(E_{HOMO} - E_{LUMO})} \quad (4)$$

$$\omega = \frac{\chi^2}{2\eta} \quad (5)$$

3. Result and Discussion

3.1. Synthesis and Characterization

The synthesis of porphyrin derivative is shown in Figure 1. The synthesis of porphyrin derivative was done in two steps. In the first step, an epoxy group containing chlorine was attached to the hydroxybenzaldehyde molecule. In the second step, the target porphyrin derivative was obtained in propanoic acid medium by using the obtained epoxy group-containing aldehyde molecule and tertiary benzaldehyde in appropriate proportions.

The peak at 3316.06 cm^{-1} shows ν(N-H) stretching. It gives a peak belonging to 1463.27 cm^{-1} ν(C=C) stretching, which can be attributed to the aromatic ring. The two weak peaks at 1042.58 cm^{-1} and 1166.17 cm^{-1} belong to the ν(C-O) and ν(C-N), respectively. The peak at 973.11 cm^{-1} is the N-H cm^{-1} peak. The peak at 724.76 also belongs to NH, but it is an out-of-plane peak. Porphyrin derivative exhibited one signal between δ = 8.90 for protons of the porphyrin core. The phenyl groups were observed at δ = 8.13, 7.83, 7.65 and 7.35 ppm.

In the aliphatic region, signals belonging to the chloroethoxy)ethoxy)ethoxy)ethoxy fragment at 8 = 4.44, 4.07, 3.89, 3.82, 3.78, and 1.28 ppm were observed. The triplet peak at 4.44 pp is the protons of CH_2 adjacent to oxygen in the phenyl ring. There are 2 in total. The triplet splitting at 4.07 ppm belongs to CH_2 adjacent to the chlorine atom and has shifted to the low area. CH_2 peaks due to oxygen appeared as singlets and 8H was at 3.78ppm. CH_3 protons in tert-butyl appeared as singlet at 1.28 ppm. Finally, there is a singlet signal at -2.78 ppm. It belongs to the internal protons (NH) of the porphyrin derivative molecule. In ^{13}C NMR, the presence of meso carbons is seen at 112 ppm and β-pyrrolic carbons in the range of 128-131 ppm. The Soret band, which is the strong absorption peak of porphyrin, appears in the range of 400-420 nm, and the Q bands, which are four weak peaks, appear in the range of 500-700 nm. These peaks are related to the π-π* electron transition of porphyrin. The absorption bands of the porphyrin derivative are as follows: 650 nm (Q-band), 592 nm (Q-band), 552 nm (Q band) 515.5 nm (Q band), 419.5 nm (Soret band).

3.2. *In Silico* Results

3.2.1. Molecular Docking

In this study, we conducted docking experiments with a newly synthesized unsymmetrical meso-aryl substituted porphyrin derivative and the target proteins EGFR (PDB ID: 1M17) and IGFR (PDB ID: 3I81) (Figure 3). We found that the compound interacted with EGFR and IGFR with a strong binding affinity of -8.6 kcal/mol and -7.2 kcal/mol, respectively (Table 1). Since EGFR and IGFR have crucial roles in cancer cell proliferation and metastasis, their suppression by strong binding of an efficient anti-cancer drug is of great importance. The binding affinities higher than -6.0 kcal/mol are considered strong bindings including many hydrogen bonds [31]. The compound established one conventional hydrogen bond with ILE854, one carbon hydrogen bond with PRO853, formed electrostatic with LYS721 and ASP831, and hydrophobic interactions with PHE699, VAL702, LYS855, TRP856, ARG817, and PRO853 residues of EGFR target protein (Figure 4-a). Furthermore, there occurred two conventional hydrogen bonds with ARG1062 and THR1133, three Pi-Donor hydrogen bonds with SER1187 and ASN1188, one pi sigma interaction with THR1133, two pi-pi T-shaped interaction with TYR1136 and one pi-alkyl interaction with ARG1137 residue of IGFR target protein (Figure 4-b).

Further, for the validation of the docking study, we performed molecular docking analysis with the ligands of EGFR (PDB ID: AQ4) and IGFR (PDB ID: EBI). These ligands were considered the positive controls.

The binding affinities of the positive controls were found to have less binding affinities to their target proteins than the newly synthesized compound (-5.5 kcal/mol and 6.1 kcal/mol, respectively). Therefore, it was shown that the newly synthesized compound has more affinity to the target proteins than their ligands.

Table 1. Detailed information of molecular docking studies performed between meso-aryl substituted porphyrin derivative and target proteins.

Compound	Target Protein	Binding Affinity (kcal/mol)	Type of Interaction	Residue Information	Distance (Å)
POR-Cl	1M17	-8.6	Conventional Hydrogen Bond	ILE854	2.920
			Carbon Hydrogen Bond	PRO853	3.597
			Pi-Cation	LYS721	4.530
			Pi-Anion	ASP831	3.657
			Pi-Anion	ASP831	3.799
			Pi-Pi Stacked	PHE699	5.974
			Pi-Pi Stacked	PHE699	3.893
			Alkyl	VAL702	4.327
			Alkyl	LYS855	4.838
			Pi Alkyl	TRP856	5.214
			Pi Alkyl	ARG817	4.510
			Pi Alkyl	VAL702	5.341
			Pi Alkyl	PRO853	5.391
	3I81	-7.2	Conventional Hydrogen Bond	ARG1062	3.105
			Conventional Hydrogen Bond	THR1133	2.997
			Pi-Donor Hydrogen Bond	SER1187	3.807
			Pi-Donor Hydrogen Bond	ASN1188	3.529
			Pi-Donor Hydrogen Bond	ASN1188	3.527
			Pi Sigma	THR1133	3.842
			Pi-Pi T-shaped	TYR1136	5.355
			Pi-Pi T-shaped	TYR1136	5.496
			Pi-Alkyl	ARG1137	5.008

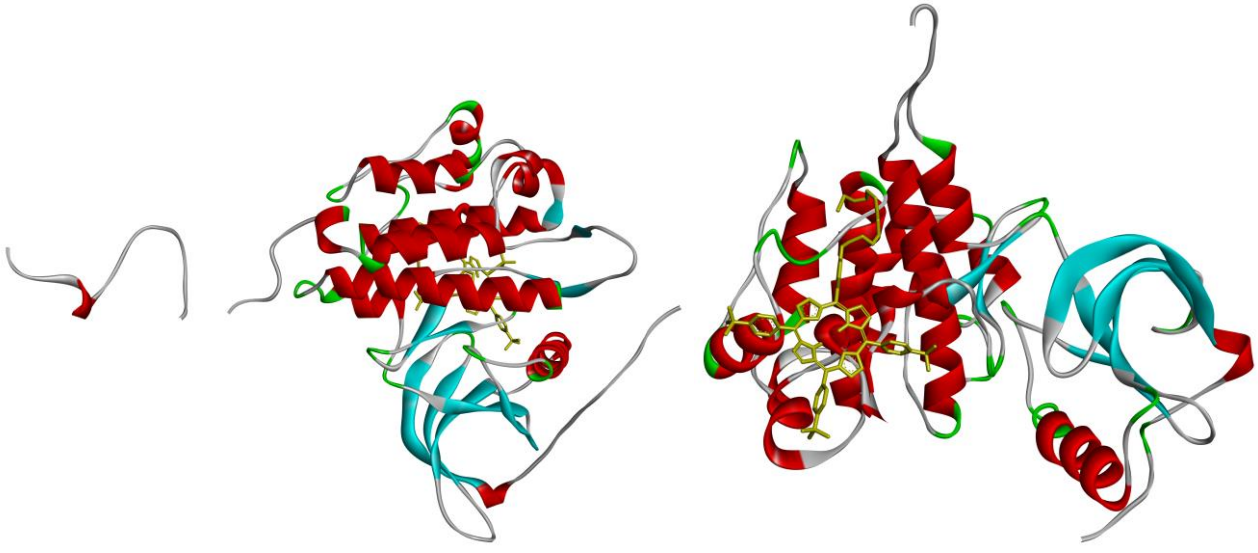

(a) (b)

Figure 3. 3D representations of molecular docking of POR-Cl and a) EGFR, b) IGFR target proteins.

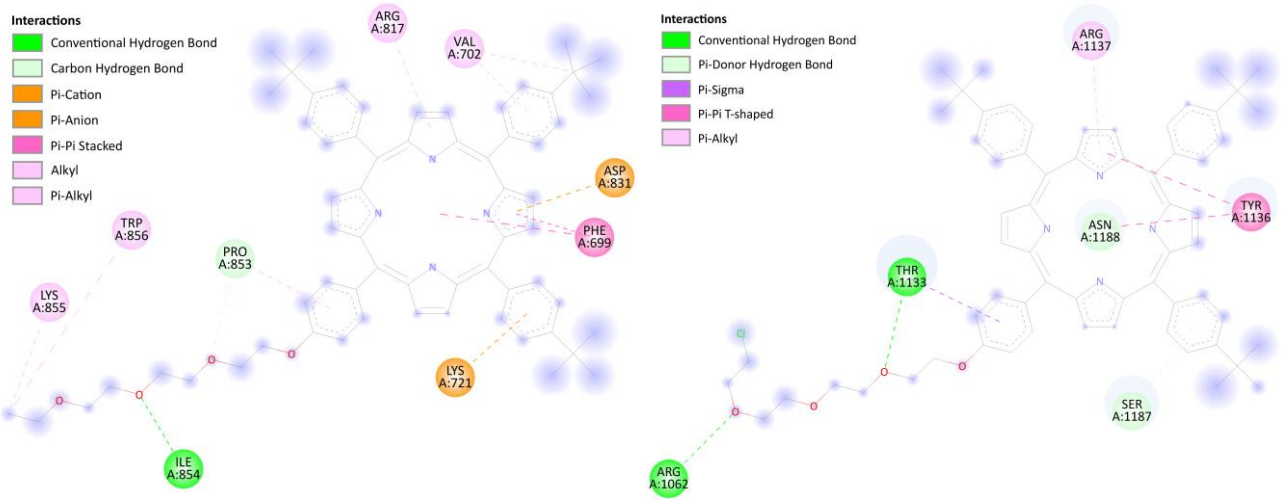

(a) (b)

Figure 4. Two-dimensional illustrations of the molecular docking of POR-Cl to a) the EGFR target protein and b) the IGFR target protein.

3.3. ADME Analysis Results

ADME is a crucial analytical method for assessing the suitability of a newly synthesized compound as a potential drug. For a compound to exhibit drug-like properties, it is essential that its bioactivity scores fall within the desired range. In this study, bioactivity scores, including G-protein coupled receptor ligand (GPCRL), ion channel modulation (ICM), kinase inhibition (KI), nuclear receptor ligand (NRL), protease inhibition (PI), and enzyme inhibition (EI), were calculated and the results are summarized in Table 2. Our findings indicate that the newly synthesized compound demonstrates moderate activity, as the scores range between -5.0 and 0 [32]. Furthermore, bioavailability which was an essential part of pharmacokinetics was evaluated by using the SwissADME website. The bioavailability score was found to be 0.57 which is in line with the ideal bioavailability condition ≥0.55 [33]. Also, since the first step of oral drug absorption is the intestinal tract, the topological polar surface area (TPSA) value was evaluated. Accordingly, it was obtained smaller than 140 Å which corresponded to an efficient intestinal absorption [34].

3.4. DFT Results

3.4.1. Geometrical Optimization

The optimization and calculations of the compound were performed using the Gaussian 09 software package [25]. Density Functional Theory (DFT) was utilized for the optimization process, employing Becke's three-parameter hybrid model (B) [35] in conjunction with the Lee, Yang, and Parr's correlation functional (LYP) [36], along with standard cc-pvdz/6-311G+(d,p) basis sets. The optimized structure of the compound is illustrated in Figure 5.

3.4.2. FMOs and Quantum Chemical Calculations

FMO analysis is a frequently used method to obtain information about the electrical characteristics of the synthesized molecules [37]. ΔE_{gap} is related to the kinetic stability and chemical reactivity of the molecule. For efficient chemical reactivity, this gap must be smaller. Therefore, since in our study the ΔE_{gap} value is very small it can be concluded that the chemical reactivity of POR-Cl is very high (Figure 6). This result implies that the compound could create strong hydrogen bonds, and hence has stability property. This result is important for supporting the strong binding of POR-Cl to EGFR and IGFR which are well-known cancer triggering receptors. The chemical reactivity descriptors of the molecules provide insight into the stability and bioactivity of the compound, as shown in Table 3. The frontier molecular orbitals (FMOs) of the POR-Cl compound are depicted in Figure 6, where positive and negative phases are represented in red and green colors, respectively. For both the HOMO and LUMO contours, electron density is predominantly localized over the main core area of the porphyrin.

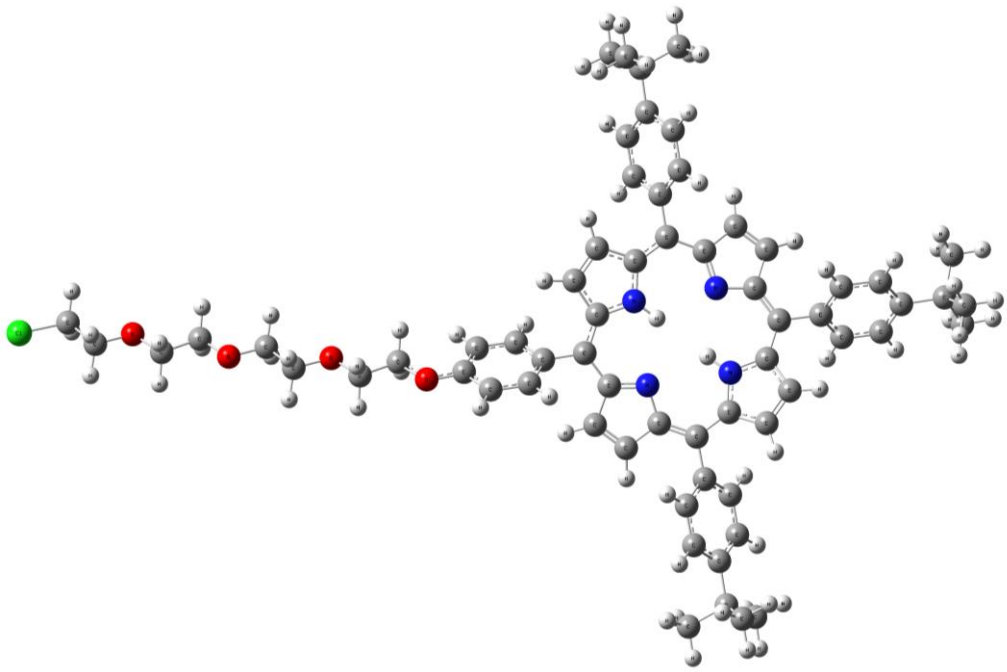

Figure 5. Optimized structure of POR-Cl compound.

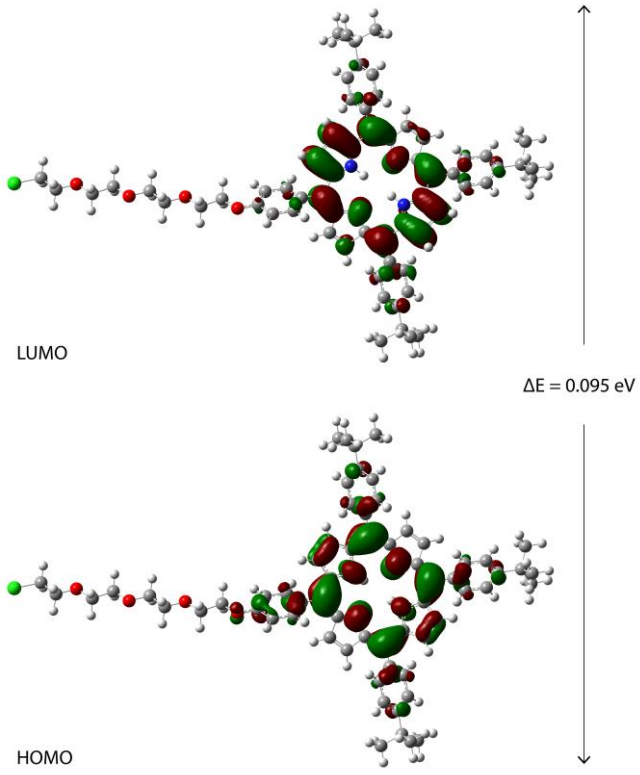

Figure 6. FMOs of POR-Cl compound

Table 2. The bioactivity scores of POR-Cl

Compound	GPCRL	ICM	KI	NRL	PI	EI
POR-Cl	-3.70	-3.78	-3.75	-3.78	-3.62	-3.72

Table 3. FMO energies and chemical reactivity descriptor values

Compound	E_{HOMO} (eV)	E_{LUMO} (eV)	ΔE_{gap} (eV)	χ	π	η	σ	ω
POR-Cl	-0.0908	-0.186	0.0952	0.138	-0.138	0.048	21.002	0.201

4. Conclusion

In conclusion, we have successfully synthesized a porphyrin derivative, which was characterized using ^{1}H NMR, ^{13}C NMR, ATR, and UV-Vis spectroscopy. Based on *in silico* analysis, the newly synthesized compound was found to be moderately active and has more affinity to the target proteins than their ligands, in particular to EGFR. Furthermore, DFT analysis revealed that the chemical reactivity of the POR-CL compound is quite high, with chemical reactivity descriptors supporting its stability and bioactivity. These findings underscore its potential as a promising candidate for targeted therapies in breast cancer treatment, benefiting from its elucidated structural, electronic, and biological properties through comprehensive characterization, in silico studies, and DFT analysis. However, since the exact underlying mechanism of the effects of the compound is unknown further studies that investigate the anticancer activities of this new compound *in vivo* are required.

5. Acknowledgement

The synthesis study received funding from the Scientific Research Projects Coordination Unit (BAP) of Muğla Sıtkı Koçman University, under project number 21/131/03/1/4. The authors wish to acknowledge the financial support provided by the Muğla Sıtkı Koçman University Scientific Research Foundation.

6. References

[1] Merhi, A., "Synthesis of new organic and organometallic Porphyrin Assemblies for Optics". Other [cond-mat.other]. INSA de Rennes, 2013. English. ⟨NNT: 2013ISAR0022⟩.

[2] Rezazgui, O., "Towards a bio-inspired photoherbicide: Synthesis and studies of fluorescent tagged or water-soluble", Doctoral dissertation, Université de Limoges, 2015.

[3] Miao, W., Zhu, Z., Li, Z., Hao, E. and Jiao, L., "Novel expanded porphyrinoids with multiple-inner-ring-fusion and/or tunable aromaticity", *Chinese Chemical Letters*, 30: 1895–1902, 2019.

[4] Luna, M. A., Moyano, F., Sereno, L. and D'Eramo, F., "Spectroscopic and electrochemical studies of high-valent water soluble manganese porphyrine", Electrocatalytic water oxidation, *Electrochimica Acta*, 135: 301–310, 2014.

[5] Marques, H. M., "Corrins and porphyrins: two of nature's pigments of life", *Journal of Coordination Chemistry*, 77(11): 1161-1210, 2024.

[6] Arambula, J. F. and Sessler, J. L.," Porphyrinoid Drug Conjugates", *Chem Perspective*, 6: 1634-1651, 2020.

[7] Senge, M. O., Sergeeva, N. N. and Hale, K. J., "Classic highlights in porphyrin and porphyrinoid total synthesis and biosynthesis", *Chem. Soc. Rev*, 50: 4730-4789, 2021.

[8] Teixeira, R., Serra, V. V., Botequim, D., Paulo, P. M. R., Andrade and Costa, S. M. B., "Fluorescence Spectroscopy of Porphyrins and Phthalocyanines: Some Insights into Supramolecular Self-Assembly, Microencapsulation, and Imaging Microscopy", *Molecules*, 26: 4264- 4289, 2021.

[9] Temelli, B., "Addition reactions of aromatic compounds to multiple bonds in the presence of metal trifluoromethanesulfonates", PhD Thesis, 2008.

[10] Severance, S. and Hamza, I., "Trafficking of heme and porphyrins in metazoa", *Chemical Reviews*, 109(10): 4596–4616, 2009.

[11] Sawicki, K. T., Chang, H.-C. and Ardehali, H., "Role of heme in cardiovascular physiology and disease", Journal *of the American Heart Association*, 4(1):1-14, 2015.

[12] Tahoun, M., Gee, C. T., McCoy, V. E., Sander, P. M. and Muller, C. E., "Chemistry of porphyrins in fossil plants and animals", RSC *Advances*, 11: 7552–7563, 2021.

[13] Tian, Z., Li, H., Liu, Z., Yang, L., Zhang, C., He, J., Ai, W. and Liu, Y., Enhanced Photodynamic Therapy by Improved Light Energy Capture Effciency of Porphyrin Photosensitizers, *Current Treatment Options in Oncology,* 24: 1274- 1292, 2023.

[14] Purtaş, S., Köse, M., Tümer, F., Tümer, M., Gölcü, A. and Ceyhan, G., "A novel porphyrin derivative and its metal complexes: Electrochemical, photoluminescence, thermal, DNA-binding, and superoxide dismutase activity studies", *Journal of Molecular Structure*, 1105: 293–307, 2016.

[15] Giovannetti, R., "The use of spectrophotometry UV-Vis for the study of porphyrins", *In Macro to Nano Spectroscopy*, 87–108, 2012.

[16] Lucantoni, L., Magaraggia, M., Lupidi, G., Ouedraogo, R. K., Coppellotti, O., Esposito, F., Fabris, C., Jori, G and Habluetzel, A., "Novel, meso-substituted cationic porphyrin molecule for photo-mediated larval control of the dengue vector Aedes aegypti", *PLoS ONE*, 5(12: e1434, 2011.

[17] Kurniawan, F., Miura, Y., Kartasasmita, R. E., Yoshioka, N., Mutalib, A. and Tjahjono, D. H., "In silico study, synthesis, and cytotoxic activities of porphyrin derivatives", *Pharmaceuticals*, 11(8): 1-18, 2018.

[18] Seyfried, T. N., Flores, R. E., Poff, A. M. and Agostino, D. P., "Cancer as a metabolic disease: Implications for novel therapeutics", Carcinogenesis, 35: 515–527, 2014.

[19] Siegel, R. L., Miller, K. D. and Jemal, A., "Cancer statistics", *CA: A Cancer Journal for Clinicians*, 67(1): 7–30, 2017.

[20] Sarikavakli, N., Genç, O., Çaliskan, Ş. G. and Erol, F., "Molecular docking, HOMO-LUMO, and quantum chemical computation analysis of anti-glyoximehydrazone derivatives containing pyrazolone moiety and their transition metal complexes", *Journal of the Indian Chemical Society*, 100(5): 100981, 2023.

[21] Hiroto, S., Miyake, Y. and Shinokubo, H., "Synthesis and functionalization of porphyrins through organometallic methodologies", *Chemical Reviews*, 117: 2910–3043, 2017.

[22] Urbani, M., Grätzel, M., Nazeeruddin, M. K. and Torres, T., "Meso-substituted porphyrins for dye-sensitized solar cells", *Chemical Reviews*, 114: 12330–12396, 2014.

[23] Wu, L. and Qu, X., "Cancer biomarker detection: Recent achievements and challenges", Chemical *Society Reviews,* 44: 2963–2997, 2015.

[24] Nishida, K., Tojo, T., Kondo, T. and Yuasa, M., "Evaluation of the correlation between porphyrin accumulation in cancer cells and functional positions for application as a drug carrier", Scientific Reports, 11: 2046, 2021.

[25] Charisiadis, A., Nikolaou, V., Karikis, N., Giatagana, C., Chalepli, K., Ladomenou, K., Biswas, S., Sharma, G. D. and Coutsolelos, A. G., "Two new bulky substituted Zn porphyrins bearing carboxylate anchoring groups as promising dyes for DSSCs", *New Journal of Chemistry*, 40: 5930–5941, 2016.

[26] Bera, R., Chakraborty, S., Nayak, S. K., Jana, B. and Patra, A., "Structural insight and ultrafast dynamics of 2D porphyrin nanostructures", *The Journal of Physical Chemistry C*, 123: 15815–15826, 2019.

[27] Fadda, A. A., El-Mekawy, R. E., El-Shafei, A., Freeman, H. S., Hinks, D. and El-Fedawy, M., "Design, Synthesis, and Pharmacological Screening ofNovel Porphyrin Derivatives" *Journal of Chemistry*, 2013.

[28] Trott, O. and Olson, A. J., "AutoDock Vina: Improving the speed and accuracy of docking with a new scoring function, efficient optimization, and multithreading", Journal *of Computational Chemistry*, 31(2): 455–461, 2010."

[29] Molinspiration. Retrieved from www.molinspiration.com

[30] Frisch, M. J., Trucks, G. W., Schlegel, H. B., Scuseria, G. E., Robb, M. A., Cheeseman, J. R., Scalmani, G., Barone, V., Petersson, G. A., Nakatsuji, H., Li, X., Caricato, M., Marenich, A., Bloino, J., Janesko, B. G., Gomperts, R., Mennucci, B., Hratchian, H. P., Ortiz, J. V., Izmaylov, A. F., Sonnenberg, J. L., Williams-Young, D., Ding, F., Lipparini, F., Egidi, F., Goings, J., Peng, B., Petrone, A., Henderson, T., Ranasinghe, D., Zakrzewski, V. G., Gao, J., Rega, N., Zheng, G., Liang, W., Hada, M., Ehara, M., Toyota, K., Fukuda, R., Hasegawa, M., Ishida, M., Nakajima, T., Honda, Y., Kitao, O., Nakai, H., Vreven, T., Throssell, K., Montgomery, J. A., Jr., Peralta, J. E., Ogliaro, F., Bearpark, M., Heyd, J. J., Brothers, E., Kudin, K. N., Staroverov, V. N., Keith, T. A., Kobayashi, R., Normand, J., Raghavachari, K., Rendell, A., Burant, J. C., Iyengar, S. S., Tomasi, J., Cossi, M., Millam, J. M., Klene, M., Adamo, C., Cammi, R., Ochterski, J. W., Martin, R. L., Morokuma, K., Farkas, O., Foresman, J. B. and Fox, D. J. Gaussian 09, Revision A.02. Gaussian, Inc., Wallingford CT, 2016.

[31] Gligori´c, E., Igi´c, R., Teofilovi´c, B. and Gruji´c-Leti´c, N., "Phytochemical Screening of Ultrasonic Extracts of Salix Species and Molecular Docking Study of Salix-Derived Bioactive Compounds Targeting Pro-Inflammatory Cytokines". *International Journal of Molecular Sciences*. 24: 11848, 2023.

[32] Verma, A., "Lead finding from *Phyllanthus debelis* with hepatoprotective potentials", *Asian Pacific Journal of Tropical Biomedicine*, 1: 735–737, 2012.

[33] Dhaheri, Y.A., Wali, A.F., Akbar, I., Rasool, S., Razmpoor, M., Jabnoun, S. and Rashid, S., Chapter 3 - Nigella sativa, a cure for every disease: Phytochemistry, biological activities, and clinical trials, Editor(s): Andleeb Khan, Muneeb Rehman, Black Seeds (Nigella Sativa), Elsevier, Pages 63-90, 2022.

[34] Shtaiwi, A., Khan, S.U., Khedraoui, M. Alaraj, M., Samadi, A. and Chtita S., "A comprehensive computational study to explore promising natural bioactive compounds targeting glycosyltransferase MurG in Escherichia coli for potential drug development". *Scientific Reports*, 14: 7098, 2024.

[35] Becke, A., "Density-functional thermochemistry. III. The role of exact Exchange", *The Journal of Chemical Physics*, 98: 5648–5652, 1993.

[36] Lee, C., Yang, W. and Parr, R. G., "Development of the Colle-Salvetti correlation-energy formula into a functional of the electron density", *Physical Review B*, 37(2): 785–789, 1988.

[37] Sukumaran, S., Zochedh, A., Chandran, K., Sultan, A. B. and Kathiresan, T., "Exploring the co-activity of FDA-approved drug gemcitabine and docetaxel for enhanced anti-breast cancer activity: DFT, docking, molecular dynamics simulation, and pharmacophore studies", *International Journal of Quantum Chemistry*, 124(4): e27359, 2024.